Trends in Biomaterials and Artificial Organs

sbaoi

Original Article

www.sbaoi.org/tibao

# Hip Implant: CAD Modelling and Static Analysis

Gajanan Damodhar Mandavgade[1], Tushar Ramkrishna Deshmukh[2]

[1]Department of Mechanical Engineering, Sipna College of Engineering & Technology, Badnera Road, Amravati 444701, Maharashtra, India
[2]Department of Mechanical Engineering, Prof. Ram Meghe Institute of Technology & Research, Anjangaon Bari Road, Badnera, Amravati 444701, Maharashtra India

*Received 14 July 2019*
*Accepted 3 September 2019*
*Published online 20 December 2019*

The purpose of this research had been to develop standard hip implant and analyze stress distribution in implant under daily activity by using ANSYS 14.5 software. In an existing study several CAD models of a hip prosthesis with a rectangular rounded corner cross section were developed. Which were the combination of three hip profiles and eight set of implants forecast through cluster analysis in IBM SPSS software V25. A Ti-6Al-4V bio-material was used for analysis. Finite Element Analysis (FEA) of each implant was conducted for normal walking and climbing staircase activity. The selection of implant was based on total deformation, as calculated stresses were significantly lower in all cases than the yield stress of Ti-6Al-4V, thus implant was safe for the static condition. FEA is a reliable and powerful tool for stress-strain analysis of complex-shaped implants, like the artificial hip prosthesis.

© (2019) Society for Biomaterials & Artificial Organs #20-0343-19

## Introduction

Hip replacement is a clinical process in which diseased parts of the femur are replaced with artificial parts, called as the hip implant [1,2]. With the escalation in hip replacements every year, the requirement of a long-term implant design increases [3].

The tendency to intra-operative cracks and fracture, implant loosening, and bone loss arise due to stress shielding and femoral osteolysis [4]. These problems were related to a geometric mismatch between an implant and endosteal bone, as there was variability in upper femoral geometry such incorrect sized implants caused serious problem to the patient [5, 6]. To overcome these problems and to achieve proper fitment between femur and implant, it is essential to design a few standard implants based on the shape and size of the proximal femur of a population.

Several regions are important in the design of the hip implant and these regions include geometry, materials, stress distribution along the stem and micro-motion between the implant and the bone. The geometry suitability between the human bones and implant is one of the most key factors for a positive outcome. The hip profile of implant can directly control the distribution of stress around the implant and help reduce implant failure [7]. The peak stress concentrations take place at the distal and proximal ends of the implant [8]. Knowing that stress attention was more in these areas an implant can be designed to distribute stress more efficiently in these zones along the implant.

Cobalt–chromium (CoCr), stainless steel (SS 316L), and a titanium alloy (Ti6Al4V) are universally used as biomaterials. Presently, titanium-based alloys, mainly Ti-6Al-4V & Ti-6Al-7Nb, are the most regularly used materials for joint prostheses, being listed in ASTM standard as biomaterials [9].

The micro-motion between the bone and implant must be reduced because increased in micro-motion decrease the bone in-growth, which results in reducing the stability of the implant. [10]. One research exposed that micro-motion within the range of 50 – 200 μm should be controlled [11].

This study aims to evaluate the von mises stresses, total deformation, maximum and minimum principal stress distribution on the standard hip implant under daily activities like walking and climbing stairs conditions with static loading condition.

## Materials and Methods

In the present study eleven anatomical parameters of femoral prosthesis of 125 subjects (67 Male and 58 female) were measured, from their X-ray in DICOM format. These eleven parameters were grouped and put under cluster analysis in IBM SPSS Statistic software (V25) and it gave standard values of each parameter

*Coresponding author.
*E-mail address: gajananmandavgade47@gmail.com (Gajanan Damodhar Mandavgade)*

**Table 1: Forecast anatomical parameters by cluster analysis**

| AP | N | Male | | | | Female | | | |
|---|---|---|---|---|---|---|---|---|---|
| | | 1.1 | 1.2 | 1.3 | 1.4 | 1.1 | 1.2 | 1.3 | 1.4 |
| A (mm) | 106 | 55.7 | 49.5 | 48.3 | 53.4 | 50.0 | 48.4 | 44.4 | 45.7 |
| B (mm) | 106 | 36.5 | 34.0 | 31.8 | 35.2 | 29.1 | 27.7 | 26.0 | 26.9 |
| C (mm) | 106 | 50.2 | 43.6 | 40.6 | 47.1 | 43.9 | 41.5 | 39.6 | 43.1 |
| D (mm) | 106 | 70.3 | 61.2 | 56.7 | 65.8 | 59.9 | 57.2 | 52.7 | 54.9 |
| E (mm) | 106 | 51.0 | 47.4 | 43.4 | 54.4 | 58.3 | 54.1 | 44.6 | 49.8 |
| F (mm) | 106 | 32.3 | 30.3 | 27.8 | 34.8 | 38.1 | 35.3 | 29.0 | 32.4 |
| G (mm) | 106 | 22.3 | 21.2 | 19.4 | 23.4 | 26.5 | 24.3 | 20.2 | 22.3 |
| H (mm) | 106 | 16.2 | 15.1 | 13.8 | 16.9 | 19.8 | 18.9 | 15.1 | 17.4 |
| I (mm) | 106 | 14.3 | 13.3 | 12.2 | 15.2 | 17.2 | 16.4 | 13.1 | 14.8 |
| J (mm) | 106 | 12.3 | 11.5 | 10.5 | 13.2 | 14.8 | 12.1 | 11.4 | 13.6 |
| M (deg) | 106 | 141.0 | 122.0 | 125.0 | 133.0 | 135.5 | 130.5 | 120.0 | 125.0 |

shown in Table 1, based on these values 8 (4 for male & 4 for female) standard sizes implants design was possible. [12]

## CAD Modelling

To optimize implant design three different hip profiles were used shown in Fig.1, Hip profile 1 had a straight stem with a radius on the lateral side near the proximal end. Hip profile 2 increased the diameter and arc length of the profile on lateral sides of the stem. Lastly, Hip profile 3 eliminated the radius on the lateral side and replaces it with a surrounded shoulder [3]

A Pro-E 4.0 CAD modeling software was used to generate 3D solid models of hip implants. These three hip profiles combined with the eight standard sizes design (forecast by cluster analysis) to create twenty-four different hip implant designs. The same is shown below in Fig.2

### Finite Element Analysis

It's assumed that in synovial joints friction was negligible, and the pressure was not hydro-static. Under these assumptions, the stresses on the articular surface were normal stresses and were proportional to the normal forces transmitted from one articulating element to the other. In addition to that, attention would be given only on the supporting stance phase of the gait, because this denotes the position of maximum articular stress. Each of the implant designs was analyzed using the material properties of Ti6Al4V given in Table 2.

According to Dowson [15] there are certain 22 muscles acting to move the femur, but in the current finite element model only two muscles were considered; the abductor muscle group (gluteus medius and gluteus minimus) and the iliotibial band. They act to prevent and stabilize the upper body during the one-legged stance phase of walking.

As three hip profiles combined with the eight standard size implants, it provided twenty-four different hip implant. These implants evaluated for two conditions (i.e normal walking and climbing staircase) and generated a total of 48 cases. For understanding the study male implant 1.1 with profile 1 is taken as a sample.

### Mesh Generation and Boundary Conditions

Software ANSYS 14.5 was used for Finite Element Analysis. The four nodes tetrahedral element was chosen to reduce the calculating time. The hip implant model had a total of 14507 nodes and 8257 elements. Mesh implant model is shown in Fig.3. Mesh generation of each model was generated by ANSYS 14.5.

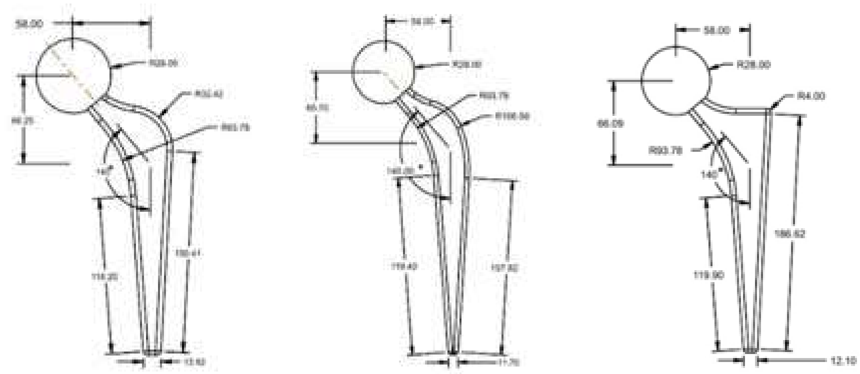


**Figure 1: Hip profile - 1 (left): Hip profile - 2 (centre) and Hip profile - 3 (right)**

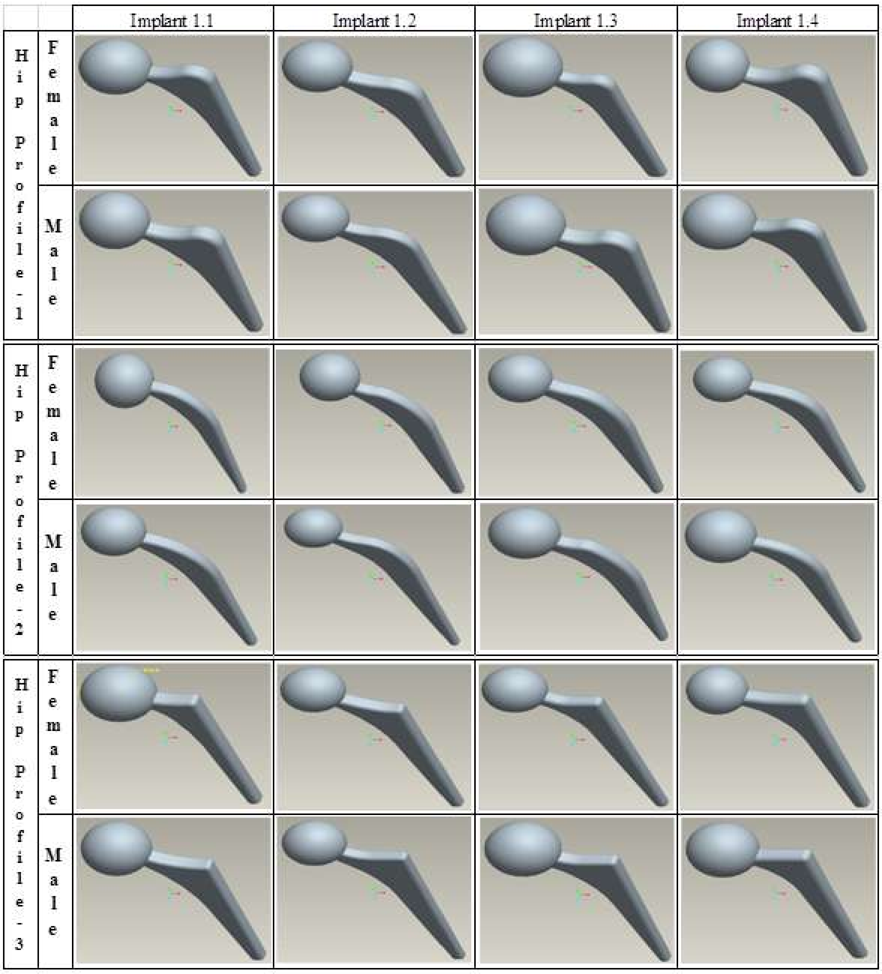


**Figure 2: Twenty four CAD models of implant for three hip profiles**

The implant was fully fixed at the distal end, and body weight acting on the tip of the femoral head and muscular force acted on the proximal end. The magnitude of the load to the hip during gait was up to 4.2 times body weight. For a zero-degree pelvic angle, the applied load was at approximately 20 degrees to the shaft of the femur [16]. For the same pelvic angle, the abductor muscle load was 1.5 times body weight and applied at an angle of 20° to the vertical over the proximal end of the greater trochanter. The iliotibial muscle load was 0.36-time body weight and applied parallel to the shaft of the femur in a distal direction shown in Fig.4. [17]. The static load on a femoral head of hip and its muscles were calculated for a person weighing 85kg. [9, 20]. Total load on Hip implant under normal walking and climbing staircase activity for static analysis were tabulated in Table 3.

## Results

Maximum Von-mises stress, Maximum and Minimum principal stresses, and Total Deformation were measured for static walking and static climbing staircase. The result for male implant 1.1 with profile 1 is shown in Fig. 5 and 6. The result of all 24 cases of static walking and 24 cases of static climbing was tabulated in Table 4 and 5 resp.

The selection process of an implant was based on total deformation, because calculated stresses were significantly lower in all cases than the yield stress of Ti-6Al-4V (860 Mpa). For both walking and staircase climbing cases the maximum von mises stress for static condition did not reach to yield strength of hip prosthesis, thus implant was safe for the static condition. Once FEA and comparison

**Table 2: Mechanical Properties of Metallic Biomaterials [13,14]**

| Material | Young's Modulus (GPa) | Yield Strength (MPa) | Tensile Strength (MPa) | Fatigue Limit (MPa) | Poisson Ratio | Density (g/cm$^3$) |
|---|---|---|---|---|---|---|
| SS 316 L | 190 | 221–1,213 | 586–1,351 | 241–820 | 0.30 | 7.9 |
| Co-Cr alloys | 210-253 | 448–1,606 | 655–1,896 | 207–950 | 0.30 | 8.5 |
| Ti-6Al-4V | 116 | 710–834 | 765–903 | 620 | 0.32 | 4.4 |
| Cortical bone | 15 - 30 | 30 - 70 | 70–150 | … | 0.30 | 2.0 |

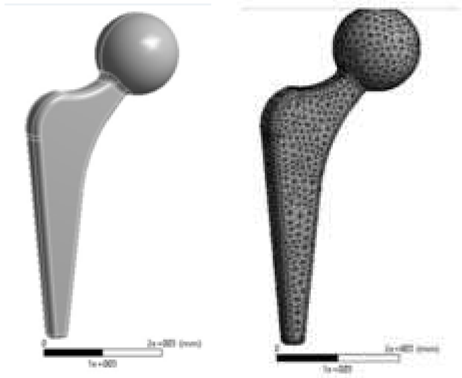

**Figure 3: CAD models of male implant 1.1 with profile-1 (left) and meshing of same model (right).**

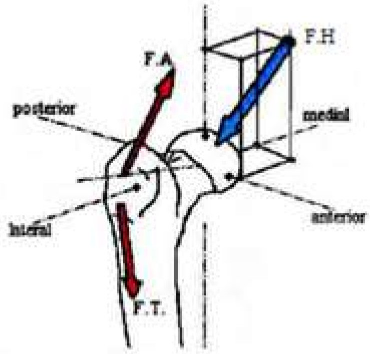


**Figure 4: Femoral bone and muscles consider to be acting load. FH: represent force on femoral head, F.A: Force on abductor muscle, and F.T: force on ilio-tibial**

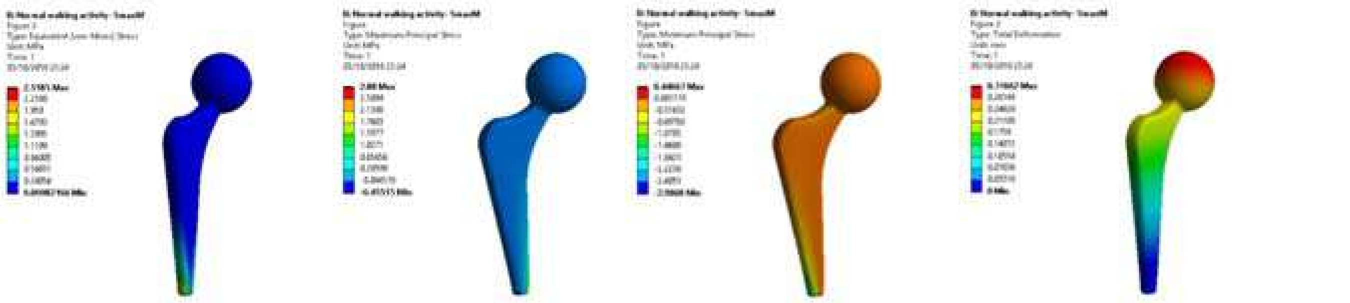

**Figure 5: (A) Maximum Von mises stress, (B) Maximum principal stresses (C) Minimum principal stresses, and (D) Total Deformation of Male implant 1.1 with profile 1 for normal walking activity.**

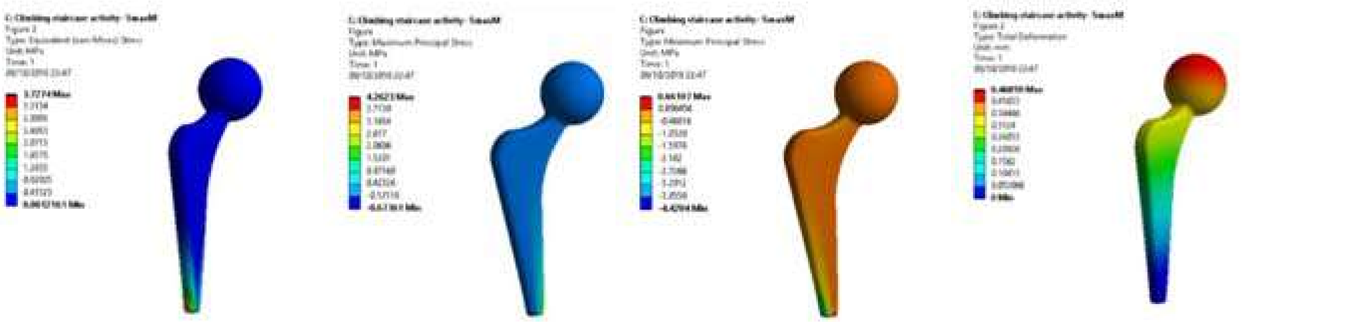

**Figure 6: (A) Maximum Von mises stress, (B) Maximum principal stresses (C) Minimum principal stresses, and (D) Total Deformation of Male implant 1.1 with profile 1 for Staircase climb activity**

**Table 3: Load on implant for static analysis**

| Location on implant where load applied | Total Body Weight (KG) | Normal walking (NW) | | Climb Staircase (CS) | |
|---|---|---|---|---|---|
| | | Body Wt. (%) | Load (N) | Body Wt. (%) | Load (N) |
| Femoral Head | 85 | 420 | 3502.2 | 621 | 5183.2 |
| Abductor Muscles | 85 | 150 | 1250.8 | 222 | 1851.1 |
| IlioTibial Band | 85 | 36 | 300.2 | 53 | 444.3 |

**Table 4: FEA result for normal walking activity**

| | Observation | Male | | | | Female | | | |
|---|---|---|---|---|---|---|---|---|---|
| | | 1.1 | 1.2 | 1.3 | 1.4 | 1.1 | 1.2 | 1.3 | 1.4 |
| **Hip Profile 1** | Von Mises Stress (Mpa) | 3.102 | 3.201 | 11.216 | 4.659 | 2.626 | 4.054 | 4.644 | 10.622 |
| | Maximum Principal Stress (Mpa) | 3.117 | 3.220 | 10.614 | 4.660 | 3.078 | 3.719 | 5.500 | 11.419 |
| | Minimum Principal Stress (Mpa) | 0.617 | 0.312 | 1.437 | 0.565 | 0.392 | 0.416 | 2.083 | 1.477 |
| | Total Deformation (mm) | 0.677 | 0.387 | 0.598 | 0.448 | 0.262 | 0.297 | 0.427 | 1.149 |
| **Hip Profile 2** | Von Mises Stress (Mpa) | 8.081 | 1.748 | 3.511 | 10.134 | 6.550 | 14.656 | 12.251 | 14.313 |
| | Maximum Principal Stress (Mpa) | 8.841 | 1.606 | 3.609 | 10.251 | 6.291 | 15.182 | 11.777 | 15.850 |
| | Minimum Principal Stress (Mpa) | 0.942 | 0.045 | 0.045 | 0.903 | 0.957 | 2.510 | 1.227 | 0.158 |
| | Total Deformation (mm) | 2.692 | 11.217 | 7.166 | 1.329 | 0.916 | 1.661 | 1.484 | 1.663 |
| **Hip Profile 3** | Von Mises Stress (Mpa) | 0.480 | 8.500 | 5.780 | 6.401 | 0.383 | 3.091 | 10.003 | 10.807 |
| | Maximum Principal Stress (Mpa) | 0.418 | 8.655 | 7.014 | 6.467 | 0.289 | 15.282 | 1.109 | 10.949 |
| | Minimum Principal Stress (Mpa) | 0.447 | 1.032 | 0.769 | 0.828 | 0.019 | 1.605 | 10.327 | 0.891 |
| | Total Deformation (mm) | 3.564 | 1.735 | 0.712 | 0.864 | 0.154 | 2.053 | 1.285 | 1.576 |

**Table 5: FEA result for staircase climbing activity**

| | Observation | Climbing Staircase | | | | | | | |
|---|---|---|---|---|---|---|---|---|---|
| | | Male | | | | Female | | | |
| | | 1.1 | 1.2 | 1.3 | 1.4 | 1.1 | 1.2 | 1.3 | 1.4 |
| **Hip Profile 1** | Von Mises Stress (Mpa) | 4.590 | 4.738 | 16.599 | 6.895 | 3.886 | 6.000 | 6.873 | 15.721 |
| | Maximum Principal Stress (Mpa) | 4.612 | 4.765 | 15.708 | 6.897 | 4.555 | 5.504 | 8.140 | 16.900 |
| | Minimum Principal Stress (Mpa) | 0.913 | 0.462 | 2.127 | 0.836 | 0.580 | 0.615 | 3.082 | 2.187 |
| | Total Deformation (mm) | 1.002 | 0.573 | 0.885 | 0.663 | 0.388 | 0.440 | 0.632 | 1.701 |
| **Hip Profile 2** | Von Mises Stress (Mpa) | 11.960 | 2.587 | 5.197 | 14.999 | 9.693 | 21.691 | 18.129 | 21.182 |
| | Maximum Principal Stress (Mpa) | 13.214 | 2.377 | 5.342 | 15.172 | 9.310 | 22.469 | 17.428 | 23.458 |
| | Minimum Principal Stress (Mpa) | 1.394 | 0.067 | 0.066 | 1.337 | 1.417 | 3.714 | 1.815 | 0.234 |
| | Total Deformation (mm) | 3.985 | 16.601 | 10.606 | 1.967 | 1.355 | 2.458 | 2.195 | 2.461 |
| **Hip Profile 3** | Von Mises Stress (Mpa) | 0.711 | 12.581 | 8.867 | 9.474 | 12.039 | 19.374 | 15.286 | 15.997 |
| | Maximum Principal Stress (Mpa) | 0.619 | 12.810 | 10.378 | 9.570 | 13.018 | 22.616 | 14.806 | 16.206 |
| | Minimum Principal Stress (Mpa) | 0.017 | 1.527 | 1.137 | 1.226 | 1.634 | 2.376 | 1.642 | 1.318 |
| | Total Deformation (mm) | 5.275 | 2.568 | 1.053 | 1.279 | 2.399 | 3.038 | 1.901 | 2.333 |

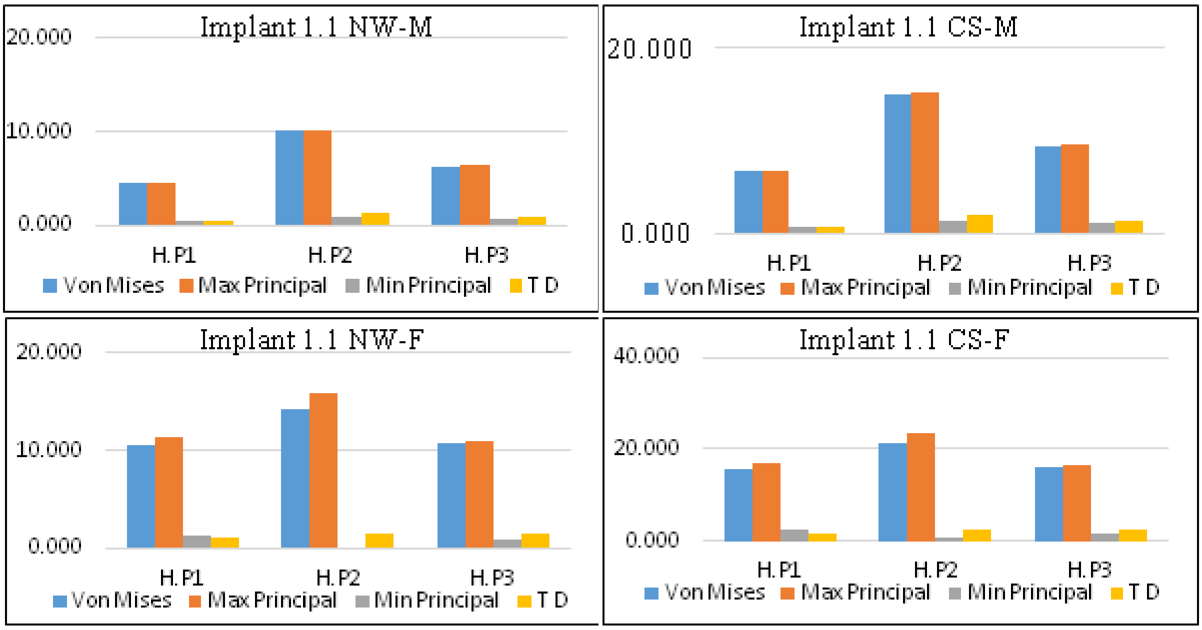


**Figure 7: Comparison between thee profiles used for male (M) and female (F). NW-normal walking, CS - staircase climbing activity**

between thee profiles carried out following outcomes were disclosed.

For both normal walking and staircase climbing cases hip implants 1.1, 1.2, 1.3, 1.4 with profile 1 were finalized for the male because hip profile 1 had less deformation as compared to profile 2 and 3. In case of female the implant 1.2 had less deformation with profile 3 than remaining two profiles, hence implant 1.2 was confirmed with profile 3 and remaining implants 1.1, 1.3, 1.4 with profile 1 was confirmed for normal walking activity and for staircase climbing activity hip implants 1.1, 1.2, 1.3, 1.4 with profile 1 was finalized.

Comparison between three hip profiles was recorded from 16 graphs, few plots of those graphs are shown in Fig 7. All graphs are not shown in this article, as it may seem to be the replication of similar plots. These plots reflect the pattern of hip profile comparison.

## Discussion

The stress distribution analysis using the finite element method is widely accepted as a useful technique to evaluate the biomechanical behaviors of orthopedic implants under a certain load condition. Simulation of mechanical behavior of hip implants under static load was performed. Calculated Von Mises stresses, Maximum and Minimum stresses were significantly lower than yield stresses of Ti-6Al-4V. A finite element study evaluated six different types of femoral stem cross sections and showed that the stress concentration varies according to the cross-section of the femoral stem [19]. The cross section for the implant used in the current study was rectangular with rounded corner. Several studies [21, 22, 23, 24] have considered different values of forces as applied to the femoral head. There have been a lot of choices regarding the selection of forces and their point of application. Most of these studies have considered femur with simple loading condition with or without abductor muscle force. In addition to this, the magnitude of force and angle at which the force is applied is different in every study. The current study considered the femur head to be loaded with abductor muscle and iliotibial muscles force and simulated a different force in different activities applied at 20°, similar to the one of the angles considered by [16, 17, 18, 19].

FEA is a reliable and powerful tool for stress-strain analysis of complex-shaped implants, like the artificial hip. The approach used by the study might be applicable for designing new implants and redesigning existing implants for the Indian population. The outcome of the current study achieved proper fitment because they were developed on the anthropometry of a respective population and reduces the chance of revision surgery. It may reduce operating time and achieve successful positioning in hip joint

## Conclusion

It can be concluded that the application of the finite element method (FEM) is a good alternative approach to provide preliminary results and an overview of the mechanical properties of potential implant models. For both activity male hip implants, 1.1, 1.2, 1.3 and 1.4 with profile 1 was ideal. For normal walking activity female implant 1.2 with profile 3 was best, and remaining implants 1.1, 1.3, 1.4 with profile 1 was confirmed and for staircase climbing activity hip implants 1.1, 1.2, 1.3, 1.4 with profile 1 was finalized.

## References

1. J.B. Park: Hip Joint Prosthesis Fixation-Problems and Possible Solutions. The Biomedical Engineering Handbook: Second Edition. CRC Press LLC. 2000. 46.1 - 46.3.
2. N.K. Jeffrey: Total joint replacement in osteoarthritis. Best Practice & Research Clinical Rheumatology., 20, 1145–153(2006).
3. A.L. Sabatini, T. Goswami: Hip implants VII: Finite element analysis and optimization of cross-sections. Science Direct Materials and Design., 29, 1438–1446(2008).
4. S. Chatterjee, U. Ghosh, S. Majumder, A. Choudhury, S. Pal: Customization of Design for Hip Implants. 58-62.
5. W.L. Bargar. Shape the implant to the pa-tient. A rationale for the use of

custom fit cement-less total hip implants. Clinical Orthopaedics & Related Research., 249, 73–78(1989).
6. P.C. Noble, J.W. Alexander, L.J. Lindahl, D.T. Yew, W.M. Granberry, H.S. Tullos: The anatomic basis of femoral component design. Clinical Orthopaedics & Related Research., 235, 148–165(1998).
7. E. Pyburn, T. Goswami: Finite element analysis of femoral components paper III – hip joints. Mater Des., 25(8), 705–13(2004).
8. H. Yildiz, F. Chang, S. Goodman: Composite hip prosthesis design. II. Simulation. Journal Biomed Mater Res., 39(1), 102–19(1998).
9. C. Katarina, A. Sedmak, A. Grbovic, U. Tatic, S. Sedmak, B. Djordjevic: Finite element modeling of hip implant static loading. International Conference on Manufacturing Engineering and Materials, ICMEM, 2016. 6-10, June 2016.
10. D. Gebauer, H.J. Refior, M. Haake: Micromotions in the primary fixation of cementless femoral stem prostheses. Arch Orthop Traumatol Surg., 108, 300–7(1989).
11. J. Orlik, A. Zhurov, J. Middleton: On the secondary stability of coated cementless hip replacement: parameters that affected interface strength. MediEng Phys., 25 (10), 825–31(2003).
12. G. Mandavgade, T. Deshmukh: Standard hip implant by cluster analysis of anthropometric parameters of femur. Journal of Med. Sci., 19, 11-16(2018).
13. J.B. Brunski: Metals, in B.D. Ratner, A.S. Hoffman, F.J. Shoen, and J.E. Lemons (eds.), Biomaterials Science: An Introduction to Materials in Medicine, Academic Press, San Diego. 37–50 (1996).
14. H. Katoozian, T. Davy: Effects of loading conditions and objective function on three-dimensional shape optimization of femoral components of hip endoprostheses. Med EngPhys.,1 22(4), 243–51(2000).
15. D. Dowson, Bio-mechanics of the lower limb, In An introduction to biomechanics of joints and joint replacements (Edited by Dowson, D. and Wright, V.), MEP, London, 1981. 68-73.
16. J.P. Paul: Approaches to design. Force actions transmitted by joints in the human body. Proc. R. Soc. Lond. B., 192, 163-172 (1976).
17. M.J. Fagan, A.J.C. Lee: Material selection in the design of the femoral component of cemented total hip replacements. Clinical Materials., 1, 151-167 (1986).
18. N.L. Svensnson, S. Valliappan, R.D. Wood: Stress analysis of human femur with implanted chamly prosthesis. Journal of Biomechanics., 10, 581-588 (1977).
19. G. Bergmann, G. Deuretzbacher, M. Heller, F. Graichen, A. Rohlmann, J. Strauss, G. Duda: Hip contact forces and gait patterns from routine activities. J. Biomech., 34, 859–871(2001).
20. D. Bennett, T. Goswami: Finite element analysis of hip stem designs. Materials and Design., 29, 45–60(2008).
21. Z. Yosibash, N. Trabelsi, C. Milgrom: Reliable simulations of the human proximal femur by high-order finite element analysis validated by experimental observations. Journal of Biomechanics., 40, 3688–3699 (2007).
22. J.A. Simoes, M.A. Vaz, S. Blatcher, M. Taylor: Influence of head constraint and muscle forces on the strain distribution within the intact femur. Journal of Medical Engineering & Physics., 22, 453–459 (2000).
23. L. Cristofolini, M. Viceconti, A. Toni, A. Giunti: Influence of thigh muscles on the axial strains in a proximal femur during early stance in gait. Journal of Biomech., 28, 617–624 (1995).
24. M.E. Taylor, K.E. Tanner, M.A.R. Freeman, A.L. Yettram: Stress and strain distribution within the intact femur: compression or bending. Journal of Medical Engg. & Phy., 18, 122–131 (1996).